Probing the Cytochrome *c* Peroxidase−Cytochrome *c* Electron Transfer Reaction Using Site Specific Cross-Linking†

Helen S. Pappa,‡ Sherareh Tajbaksh,‡ Aleister J. Saunders,§ Gary J. Pielak,§ and Thomas L. Poulos*,‡

Departments of Molecular Biology & Biochemistry and Physiology & Biophysics, University of California at Irvine, Irvine, California 92717, and Departments of Chemistry and Biochemistry & Biophysics, University of North Carolina, Chapel Hill, North Carolina 27599

Received December 13, 1995; Revised Manuscript Received February 14, 1996⊗

ABSTRACT: Engineered cysteine residues in yeast cytochrome *c* peroxidase (CCP) and yeast iso-1-cytochrome *c* have been used to generate site specifically cross-linked peroxidase−cytochrome *c* complexes for the purpose of probing interaction domains and the intramolecular electron transfer reaction. Complex 2 was designed earlier [Pappa, H. S., & Poulos, T. L. (1995) *Biochemistry 34*, 6573−6580] to mimic the known crystal structure of the peroxidase−cytochrome *c* noncovalent complex [Pelletier, H., & Kraut, J. (1992) *Science 258*, 1748−1755]. Complex 3 was designed such that cytochrome *c* is tethered to a region of the peroxidase near Asp148 which has been suggested to be a second site of interaction between the peroxidase and cytochrome *c*. Using stopped flow methods, the rate at which the ferrocytochrome *c* covalently attached to the peroxidase transfers an electron to peroxidase compound I is estimated to be ≈0.5−1 s^{-1} in complex 3 and ≈800 s^{-1} in complex 2. In both complexes the Trp191 radical and not the Fe^{4+}═O oxyferryl center of compound I is reduced. Conversion of Trp191 to Phe slows electron transfer about 10^3 in complex 2. Steady state kinetic measurements show that complex 3 behaves like the wild type enzyme when either horse heart or yeast ferrocytochrome *c* is used as an exogenous substrate, indicating that the region blocked in complex 3 is not a functionally important interaction site. In contrast, complex 2 is inactive toward horse heart ferrocytochrome *c* at all ionic strengths tested and yeast ferrocytochrome c at high ionic strengths. Only at low ionic strengths and low concentrations of yeast ferrocytochrome *c* does complex 2 give wild type enzyme activity. This observation indicates that in complex 2 the primary site of interaction of CCP with horse heart and yeast ferrocytochrome *c* at high ionic strengths is blocked. The relevance of these results to the pathway versus distance models of electron transfer and to the interaction domains between peroxidase and cytochrome *c* is discussed.

Cytochrome *c* peroxidase (CCP)[1] catalyzes the peroxide dependent oxidation of ferrocytochrome *c* in the following multistep reaction (Yonetani, 1976).

$$\mathrm{CCP(Fe^{3+}\ Trp) + H_2O_2 \rightleftarrows \underset{\text{compound I}}{CCP(Fe^{4+}{=}O\ Trp^{\bullet+})}}$$

$$\mathrm{CCP(Fe^{4+}\ Trp^{\bullet+}) + cyt.c(Fe^{2+}) \rightarrow \underset{\text{compound I}}{} \underset{\text{compound II}}{CCP(Fe^{4+}{=}O\ Trp) \text{ or } CCP(Fe^{3+}\ Trp^{\bullet+})}}$$

$$\mathrm{\underset{\text{compound II}}{CCP(Fe^{4+}{=}O\ Trp) \text{ or } CCP(Fe^{3+}\ Trp^{\bullet})} + cyt.c(Fe^{2+}) \rightarrow CCP(Fe^{3+}\ Trp)}$$

First, CCP reacts with hydrogen peroxide to form compound I. The two peroxide-oxidizing equivalents are stored as the oxyferryl, Fe^{4+}═O, center and as a cationic Trp191 radical (Sivaraja et al., 1989). Then in two successive one-electron transfer steps, compound I is reduced back to the ferric (Fe^{3+}) resting state by two ferrocyt.c molecules.

One unanswered question in this mechanism is whether CCP has two separate sites of interaction with cyt.c that are electron transfer competent. Fluorescence-quenching experiments (Leonard & Yonetani, 1974), spectrophotometric titrations (Erman & Vitello, 1980), and NMR studies (Moench et al., 1992) are consistent with a 1:1 ratio of the CCP:cyt.c complex. Quantitative static and time-resolved singlet energy transfer measurements as well as fluorescence anisotropy measurements are consistent with two similar and rapidly interconverting sites that exhibit small differences in Fe−Fe distance or heme−heme angle (McLendon et al., 1993).

In contrast to the one-site model, the biphasic steady state kinetics observed with eukaryotic cytochrome *c* species as substrates were attributed to the reaction of cyt.c at two distinct sites on CCP (Kang et al., 1977). Moreover, direct physical evidence consistent with a two-site model has accumulated. Stemp and Hoffman (1993) measured both triplet state quenching of the of zinc-substituted CCP binding to cyt.c and the fraction of that quenching that is due to

† This research was supported in part by grants from the National Institutes of Health.

* To whom correspondence should be addressed at the Department of Physiology & Biophysics. E-mail: poulos@uci.edu. Fax: (714) 824-8540.

‡ University of California at Irvine.

§ University of North Carolina.

⊗ Abstract published in *Advance ACS Abstracts,* April 1, 1996.

[1] Abbreviations: CCP, cytochrome *c* peroxidase; CCPI, CCP compound I; CCPII, CCP compound II; A128CCP, CCP with the naturally occurring Cys128 converted to Ala; cyt.c, cytochrome *c*; complex 2, intermolecular disulfide between Cys290 of CCP and Cys73 of cyt.c designed to mimic the Pelletier−Kraut structure of the noncovalent complex; complex 3, intermolecular disulfide bridge between Cys149 of CCP and Cys79 of cyt.c designed to block a predicted site of interaction on CCP centered near Asp148; cyt.c, cytochrome c; TN, turnover number in units of s^{-1}.

0006-2960/96/0435-4837$12.00/0 © 1996 American Chemical Society

electron transfer. These results are consistent with a model where CCP has a low-affinity site for cyt.c that is efficient in electron transfer and a high affinity site that exhibits low electron transfer rates. Following this work, reverse Stern−Volmer titrations performed by Zhou and Hoffman (1994) show that the 2:1 binding stoichiometry for the binding of cyt.c to CCP at low ionic strengths persists at high ionic strengths. Moreover, similar experiments in the presence of copper-substituted cyt.c as an electron transfer inert inhibitor support the sequential binding model where the first cyt.c binds strongly at a nonreactive domain and the second binds weakly at a reactive one, with the observed electron transfer occurring in the 2:1 species (Zhou et al., 1995). Potentiometric data at low ionic strengths also are in agreement with the 2:1 binding mechanism with two inequivalent binding sites with distinctively different ionic properties (Mauk et al., 1994). Rapid reaction kinetics also are consistent with two electron transfer sites. Depending on the experimental conditions, the most important being ionic strength, either the Fe^{4+}═O center or the Trp radical is reduced first (Hahm et al., 1993; Matthis et al., 1995).

The site of interaction identified in the crystal structure of the CCP−cyt.c noncovalent complex (Pelletier & Kraut, 1992) has been equated with the high-affinity site (Zhou & Hoffman, 1994; Mauk et al., 1994), although this site also has been equated with low electron transfer efficiency (Zhou & Hoffman, 1994). However, we recently described a specific covalent intermolecular disulfide-bridged complex between CCP−cyt.c, designated complex 2, that is designed to mimic the Pelletier−Kraut structure. This complex is very efficient in intramolecular electron transfer (Pappa & Poulos, 1995). This leaves open the possibility that CCP may have another interaction site even more efficient in electron transfer than the one proposed by the Pelletier−Kraut crystal structure.

Brownian dynamics simulations of the CCP−cyt.c complex (Northrup et al., 1987, 1988) provided some insights on alternate sites of interaction. The predicted primary site is near that observed in the Pelletier−Kraut structure, while the next best site is predicted to be centered around Asp148 of CCP. To test directly if this CCP region is important for electron transfer, we have prepared a highly specific 1:1 covalent complex that blocks the CCP−cyt.c interaction on the site proposed by Northrup et al. (1987, 1988). To engineer this complex, we replaced Lys149 of CCP and Lys79 of yeast cyt.c with cysteines and the two variants were cross-linked through a disulfide. An extensive steady state analysis for this complex 3 was performed, and the data were compared with the steady state data of our previous complex 2 designed to mimic the crystal structure of the noncovalent complex. We also have further explored intramolecular electron transfer in both complexes 2 and 3 to learn if the Fe^{4+}═O center or Trp191 radical is reduced by the covalently attached cyt.c.

MATERIALS AND METHODS

Materials. All chemicals used were of the highest grade and were also purchased from Sigma Chemical Co.

Mutagenesis. CCP mutants were constructed in the *Escherichia coli* expression plasmid PT-7 using the single-stranded mutagenesis method developed by Kunkel et al. (1987). The naturally occurring cysteine, Cys128, in CCP was converted to alanine, and this mutant is designated wild type CCP (Pappa & Poulos, 1995). Using the A128CCP single-stranded DNA, the Lys149 → Cys was constructed. The oligonucleotide used for construction of the Lys149 → Cys mutant was 5′-GCC TGA CGC TGA **TTG** CGA CGC TGG C-3′. The triple CCP mutant, Cys128 → Ala, Glu290 → Cys, and Trp191 → Phe, was constructed from the double A128/C290 mutant using the oligonucleotide 5′-GGA TAC GAA GGG CCA **TTC** GGA GCC GC-3′. The Lys79 → Cys yeast cyt.c mutant also was prepared using the methods described by Hilgen and Pielak (1991), while the Lys73 → Cys cyt.c mutant was constructed according to Pappa and Poulos (1995). Both yeast cyt.c mutants had their naturally occurring cysteine at position 102 converted to threonine (Cutler et al., 1987).

Protein Purification. Mutant and wild type CCP were expressed in *E. coli* and purified as previously described (Fishel et al., 1987; Choudhury et al., 1994). The CCP concentration was estimated spectrophotometrically using an extinction coefficient at 408 nm of 96 mM^{-1} cm^{-1}. The C73cyt.c mutant was prepared from a 180 l fermentation of *Saccharomyces cerevisiae* strain B-6748, and purified according to Cutler et al. (1987), with the modifications introduced by Pappa and Poulos (1995). The cyt.c concentration was estimated spectrophotometrically using an extinction coefficient of 106 mM^{-1} cm^{-1} at 410 nm.

Cross-Linking. The conditions for cross-linking cyt.c to CCP are described by Pappa and Poulos (1995), and the same conditions were used for both Cys73 and Cys79 cyt.c mutants. Improved yields of the 1:1 covalent complex were observed when the cyt.c was treated with DTT before cross-linking. The excess of dithiothreitol (DTT) was removed through a G25 column before the cross-linking reaction. The covalent complex was purified from the CCP and cyt.c monomers and homodimers by the method described by Pappa and Poulos (1995). The purity of the complex was estimated by sodium dodecyl sulfate−polyacrylamide gel electrophoresis (SDS−PAGE) electrophoresis. The concentration of the complex was estimated spectrophotometrically using an extinction coefficient of 200 mM^{-1} cm^{-1} at the Soret maximum.

Steady State Activity. The steady state enzyme kinetics of wild type CCP and the two 1:1 covalent complexes, using horse and yeast ferrocyt.c as substrates, were determined as described by Kang et al. (1977). The oxidation of ferrocyt.c was measured by following the change of absorbance at 550 nm in a Cary spectrophotometer at room temperature. Fully reduced ferrocyt.c was used as substrate at a concentration range of 1−20 μM. We used the Cys102 → Thr cyt.c mutant as the yeast cyt.c substrate to avoid the problem of interprotein disulfide formation and autoreduction associated with the reactive cysteine at position 102 of iso-1, cyt.c (Cutler et al., 1987). Data are presented as Eadie−Hofstee plots with the rate expressed as the turnover number (Wang & Margoliash, 1995).

For the yeast cyt.c steady state assays, 0.09−0.37 nM A128CCP and 0.08−2 nM complex 3 were used. For the horse cyt.c assays, 0.4 nM A128CCP and 0.46 nM complex 3 were used. For complex 2, slightly higher protein concentrations (1.4 and 13 nM) had to be used for the yeast and horse cyt.c assays, respectively. Initiation of the reaction

by the addition of hydrogen peroxide, rather than with enzyme, was employed to minimize any possible oxidation of the cytochromes by hydrogen peroxide. Steady state turnover values were derived by division of the initial velocity by enzyme concentration.

Stopped Flow Kinetics. Transient kinetic studies were performed with a Hi-Tech SF-51 stopped flow spectrophotometer using a 1 cm path length cell. For estimation of the rate of reduction of free C79cyt.c by ascorbate, a 4 μM C79cyt.c solution and varying concentrations of ascorbate (2−20 μM) were placed in 2.5 mL syringes. The reduction of cyt.c was followed at 416 nm. The rate of reduction of the covalently attached cyt.c in the CCP−cyt.c complex 3 was very slow and, therefore, was measured with a conventional spectrophotometer at 416 nm. All rates were determined at a final buffer concentration of 100 mM potassium phosphate (pH 6.0).

The rate of compound I formation within the covalent complexes also was determined using stopped flow spectroscopy. Complex (4 μM) was mixed with varying hydrogen peroxide concentrations (4−20 μM), and compound I formation was followed at 425 nm.

For determination of the intramolecular electron transfer rate in complex 3, the stopped flow procedure used by Pappa and Poulos (1995) was followed. In brief, one syringe contains the complex with reduced cyt.c, and the other syringe contains peroxide. Mixing results in the formation of compound I followed by intramolecular electron transfer from cyt.c to compound I. Oxidation of cyt.c was followed at 416 nm, an isosbestic point for CCP and CCP compound I. The complex 3 concentration was 6 μM, and the peroxide was added at a 5-fold excess. The buffer used was degassed 200 mM potassium phosphate (pH 6.0). To determine whether the compound I Fe^{4+}═O center or the tryptophan accepts the cyt.c electron during intramolecular electron transfer, the oxidation/reduction of the CCP heme iron was followed at 432 nm for complex 3 and 428 nm for complex 2. Both wavelengths were empirically determined in our stopped flow instrument to be an isosbestic point for cyt.c in the respective complexes. The analysis of the Trp191 → Phe complex 2 mutant was more complicated because replacement of Trp191 with Phe leads to a large absorbance drop in the Soret region, owing to formation of a compound I porphyrin π cation radical (Erman et al., 1989). Over a period of ≈0.1 s, the absorbance returns to give the characteristic Fe^{4+}═O spectrum due to porphyrin π cation radical reduction by some unknown electron donor (Erman et al., 1989). This creates difficulties in following ferrocyt.c oxidation if the time scale of ferrocyt.c oxidation is similar to that of porphyrin reduction. However, the oxidation rate of ferrocyt.c was so slow in the complex 2 Trp191 → Phe mutant that the reduction of the prophryin radical and oxidation of ferrocyt.c were well separated in time.

RESULTS

Modeling the Cross-Linked Complexes. Hypothetical models of the covalent complexes used in this study are shown in Figure 1. Complex 2, designed to mimic the Pelletier−Kraut crystal structure, has been described, and we have shown that the intramolecular electron transfer rate from cyt.c to CCP compound I is ≈800 s^{-1} (Pappa & Poulos, 1995). Complex 3 was designed to probe the possible second interaction site of CCP with cyt.c predicted by Brownian dynamics simulations to be centered on Asp148 of CCP (Northrup et al., 1987, 1988). To choose where to place Cys residues, models of CCP and cyt.c were docked manually using a graphics workstation. The location of the cyt.c cysteine residue was restricted to be near the exposed heme edge of cyt.c because an intermolecular disulfide forces the cyt.c heme edge to be oriented toward CCP. Since the exposed heme edge is generally considered to be the site for both oxidation and reduction of cyt.c, orientation of the cyt.c heme edge toward CCP should promote intramolecular electron transfer and diminish intermolecular electron transfer. Moreover, NMR experiments show that the interaction of cyt.c and CCP involves the exposed heme edge of cyt.c (Moench et al., 1992; Yi et al., 1993). Conversion of Lys79 to Cys satisfies these criteria and also has the advantage that the Cys79 cyt.c mutant has been characterized. The choice of where to place the cysteine in CCP was based on the following criterion. The cysteine residue must be close to the predicted site of interaction, Asp148, but be sterically accessible for cross-linking to Cys79 of cyt.c. Conversion of Lys149 to Cys appears to meet this criterion.

The next problem was how the cyt.c will orient relative to CCP. The five dihedral angles defining the conformation of an S−S bond, two each for the Cα−Cβ and Cβ−Sγ bonds and one for the Sγ−Sγ bond, have restricted values. For example, the Cα−Cβ , Cβ−Sγ, and Sγ−Sγ bonds are favored to be −60, −90, and −90°, respectively, for an S−S bridge with a left-handed twist (Richardson, 1981; Thorton, 1981). For a right-handed twist, these values are −60, +120, and +90° with one of the Cβ−Sγ dihedral angles being −50° (Richardson, 1981; Thorton, 1981). We examined every possible set of favored dihedral angles, many of which were eliminated on the basis of steric clashes. The four most probable orientations that both satisfy the favored dihedral angles and do not lead to steric problems are shown in Figure 1. The order of best to worst goes from top to bottom in Figure 1. This ordering is subjective and is based primarily on possible intermolecular contacts besides the S−S bond. For example, the first complex (top in Figure 1) has the tightest fit between the two molecules with a possible ionic interaction between Lys72 of cyt.c and Asp148 of CCP. Independent of the precise orientation, however, the Asp148 region of CCP cannot interact with another cyt.c molecule.

Characterization of A128C149CCP. The single cysteine residue at position 128 has been replaced by alanine and the mutant characterized in our previous work (Pappa & Poulos, 1995). Using the A128CCP mutant, a cysteine residue was introduced at position 149, and the double mutant was designated A128C149CCP. The double mutant incorporated heme, and its UV/visible absorption spectra are very similar to those of wild type CCP. The activity of the double mutant toward horse ferrocyt.c is ≈75% of the wild-type CCP activity. For the purpose of this study, the A128C149CCP mutant will be referred to as wild type.

Characterization of A128C290F191CCP. The double mutant was converted to a triple mutant by changing Trp191 to Phe to test the role of Trp191 in the intramolecular electron transfer. The triple mutant exhibits all the spectral properties expected from the Trp191 → Phe mutant, including <1% of wild type activity (Mauro et al., 1988).

Characterization of Cys79Thr102 Yeast cyt.c. The C79T102 yeast iso-1-cyt.c mutant also was characterized in terms of

FIGURE 1: Stereoscopic models of the four most likely orientations of complex 3 where Cys149 of CCP forms a disulfide bond with Cys79 of cyt.c. The location of cyt.c based on the crystal structure of the noncovalent complex (Pelletier & Kraut,1992) is labeled as crystal. This also is the most probable orientation in covalent complex 2 (Pappa & Poulos,1995). The hemes and Trp191 in CCP are shown.

redox potential and reactivity with ascorbate. We were mostly concerned about the cyt.c mutants' redox potential because any changes will affect electron transfer rates. The formal potential of the Lys79 → Cys at pH 4.6 is 292 ± 1

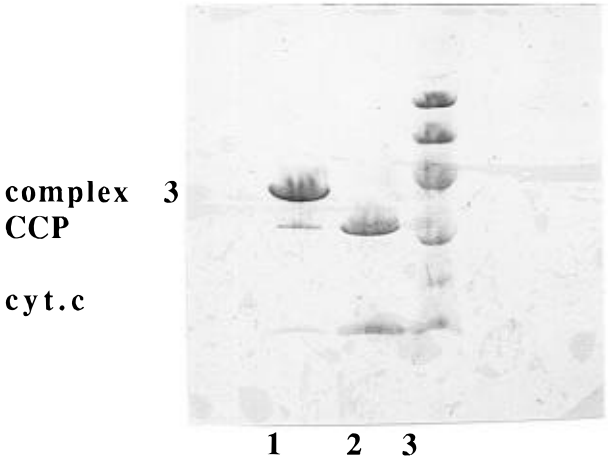

FIGURE 2: SDS−PAGE 10−15% of complex 3: lane 1, complex 3 without reducing agent; lane 2, complex 3 with reducing agent; and lane 3, molecular weight standards.

mV versus a normal hydrogen electrode. Under identical conditions the Cys102 → Thr cyt.c mutant has a formal potential of 299 ± 1 mV. The reduction rate of C79T102cyt.c by ascorbate is estimated to be 3 M^{-1} s^{-1} compared to 14 M^{-1} s^{-1} for the wild type yeast cyt.c under identical conditions.

Characterization of Complex 3. Complex 3 was prepared and purified using the protocol for complex 2 (Pappa & Poulos, 1995). Formation of the complex was followed using SDS−PAGE in the presence and absence of a reducing agent. As shown in Figure 2, complex 3 migrates as a species with an apparent molecular mass near 45 000 Da, while in the presence of a reducing agent, two bands appear, one near 12 000 and one near 32 000 Da, corresponding to the molecular masses of cyt.c and CCP, respectively. This demonstrates that complex 3 has an intermolecular disulfide. The gel also shows the presence of <5% un-cross-linked CCP and cyt.c.

Compound I Formation in Complex 3. The rate of compound I formation was determined in the stopped flow by mixing the complex with varying concentrations of peroxide and following the formation of compound I at 425 nm. CCP forms compound I with a rate constant of 3.2 × 10^7 M^{-1} s^{-1} (Erman et al., 1987), and we estimated a rate constant of 2.4 × 10^7 M^{-1} s^{-1}. Both complexes 2 and 3 react with peroxide at the same rate within experimental error. This indicates that the catalytic machinery required for compound I formation is not altered in the complex.

Rate of Cyt.c Reduction in Complex 3. The rate of cyt.c reduction is used as a probe to measure the accessibility of the cyt.c heme edge in previous covalent CCP−cyt.c complexes (Waldmeyer & Bosshard, 1985; Erman, et al., 1987; Pappa & Poulos, 1995) and noncovalent CCP−cyt.c complexes (Mochan & Nicholls, 1972). The rate of reduction of cyt.c within complex 3 was too slow to be measured in the stopped flow and therefore was estimated using conventional spectrophotometry. Complex 3 was reduced with a rate constant of 0.02 M^{-1} s^{-1} which is significantly smaller than that for complex 2 and free cyt.c, 0.17 and 5 M^{-1} s^{-1}, respectively. These results indicate that the heme in complex 3 is even more inaccessible to ascorbate than the heme in complex 2. Moreover, it enforces our modeling studies that selected for complexes where the cyt.c heme edge is oriented toward CCP. Because of the very slow reduction of the cyt.c within complex 3, it was necessary to incubate complex 3 with a large excess of ascorbate for at least 1 h to ensure total reduction before performing any further electron transfer studies.

Intramolecular Electron Transfer. In these experiments, cyt.c is reduced by ascorbate, which has no effect on CCP. The CCP−ferrocyt.c covalent complex then is mixed with H_2O_2, and depending on the wavelength, either the oxidation of ferrocyt.c or the formation/reduction of the compound I Fe^{4+}═O center is followed. The data are analyzed according to the following scheme:

$$\text{CCP}-\text{cyt.c}(Fe^{2+}) + H_2O_2 \xrightarrow{k_1} \text{CCPI}-\text{cyt.c}(Fe^{2+}) \xrightarrow{k_2} \text{CCPII}-\text{cyt.c}(Fe^{3+})$$

In this scheme, CCPI represents compound I and CCPII represents compound II. Ideally, $k_1[H_2O_2] >> k_2$ so that the rate constant we measure is k_2. For complex 2, designed to mimic the Pelletier−Kraut structure, the reaction is too fast to achieve this goal and about 75% of the reaction is over in the dead time of the instrument. Therefore, only a lower estimate of about ≈800 s^{-1} for k_2 is obtained (Figure 3A; Pappa & Poulos, 1995). Using the same procedure, the rate constant of ferrocyt.c oxidation in complex 3 is only ≈1 s^{-1} when 5 μM reduced complex 3 was mixed with a 5-fold excess of hydrogen peroxide (Figure 4). The absorbance change corresponds to approximately 80% of the value expected for complete ferrocyt.c oxidation. The rate of oxidation of the ferrocyt.c within the complex is independent of protein concentration, indicating that the electron transfer is intramolecular rather than intermolecular (Figure 4). Moreover, the oxidation rate of the ferrocyt.c is independent of hydrogen peroxide concentration, as expected.

A relevant question is whether the single ferrocyt.c electron is donated to the Fe^{4+}═O or to the tryptophan radical of compound I. The tryptophan radical is spectrophotometrically silent, and therefore, the appearance and disappearance of Fe^{4+}═O can be followed at the isosbestic point for cyt.c, near 430 nm. If only an increase near 430 nm, corresponding to the formation of the Fe^{4+}═O, is observed during the time it takes to oxidize ferrocyt.c, it is assumed that the Trp191 radical is reduced (Hahm et al., 1993; Matthis *e*t al., 1995). After mixing 4 μM complex 2 with an equimolar concentration of hydrogen peroxide, we observed the formation of the Fe^{4+}═O center of compound I at 428 nm (Figure 3A), the empirically determined isosbestic point for cyt.c in complex 2. However, there was no decrease at 428 nm during the time it takes to oxidize ferrocyt.c, demonstrating that the Fe^{4+}═O center does not receive the electron. Hence, it must be the Trp191 radical that is reduced. When this experiment was repeated with complex 3, the single ferrocyt.c electron also was delivered to the tryptophan radical rather than the Fe^{4+}═O center as shown (Figure 4).

We further probed the role of Trp191 in complex 2 by converting Trp191 to Phe. Mauro et al. (1988) showed that the Trp191 → Phe mutant blocks electron transfer in the noncovalent complex. The analysis of this reaction is more complex because, when Trp191 is converted to Phe, the species formed upon reaction with peroxide is a short-lived porphyrin π cation radical (Erman et al., 1989). The inset in Figure 3B shows the initial decrease at 416 nm due to

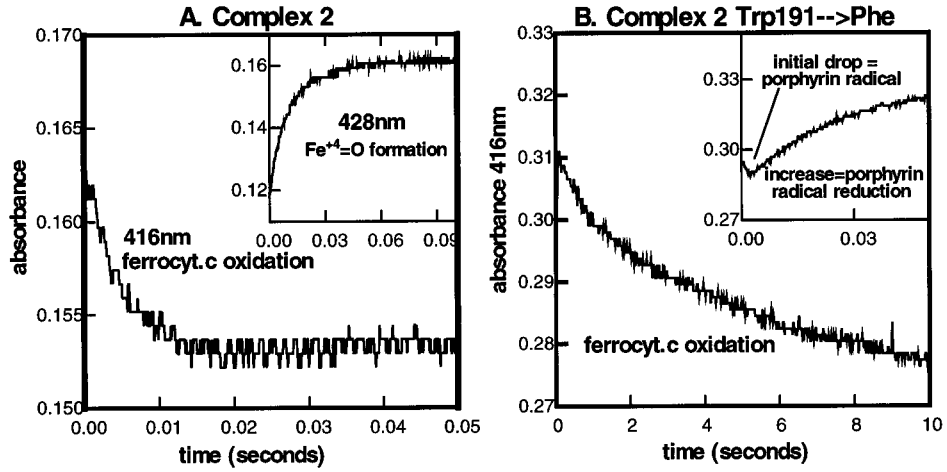

FIGURE 3: Rate of oxidation of ferrocyt.c in complex 2. The reaction is initiated by mixing peroxide with complex 2 (CCP−ferrocyt.c). (A) The trace at 416 nm represents the oxidation of ferrocyt.c by CCPI in the covalent complex 2. The trace at 428 nm (inset) shows the formation of the Fe^{4+}=O center of CCPI. Because the absorbance at 428 nm increases and is constant over the time it takes for ferrocyt.c to oxidize, it must be the Trp191 radical that is reduced in complex 2. (B) This panel is the same experiment except Trp191 of CCP in complex 2 has been converted to Phe. The inset shows the change at 416 nm over a shorter time range. The initial drop in absorbance is due to formation of a porphyrin π cation radical (Erman et al., 1989) followed by an increase in absorbance due to reduction of the porphyrin radical. Over a still longer time interval, the absorbance at 416 nm decreases due to the slow ferrocyt.c oxidation.

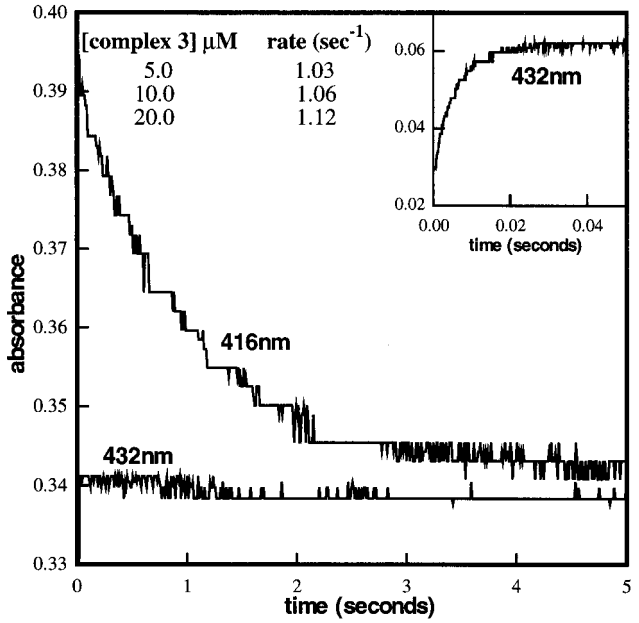

FIGURE 4: Trace at 416 nm represents the oxidation of ferrocyt.c by CCPI complex 3. The trace at 432 nm (inset) shows the rapid formation of the Fe^{4+}=O center. Because the absorbance at 432 nm is constant over the time it takes ferrocyt.c to oxidize, it must be the Trp191 radical that is reduced. Also shown is k_{obs} versus complex 3 concentration. The rate is constant from 5−20 μM complex 3, indicating that the oxidation of ferrocyt.c is an intramolecular process.

formation of the porphyrin π cation radical which then is reduced by, perhaps, an internal amino acid donor, resulting in a return of absorbance at 416 nm. The spectrum at this point resembles that of the normal Fe^{4+}=O intermediate (Erman et al., 1989) so any changes at 416 nm after reduction of the porphyrin radical are due to ferrocyt.c oxidation. As shown in Figure 3B, the absorbance at 416 nm decreases again over a longer time scale due to ferrocyt.c oxidation with a rate constant of 0.5−1.0 s^{-1}. Therefore, changing Trp191 to Phe lowers the intramolecular electron transfer rate in complex 2 by about 3 orders of magnitude, very similar to what happens in the noncovalent complex (Mauro et al., 1988).

Steady-State Kinetics. The CCP−cyt.c interaction site proposed by the Pelletier−Kraut structure is covalently blocked by a molecule of cyt.c in complex 2. In a similar manner, the site proposed on the basis of electrostatic and Brownian dynamics calculations (Northrup et al., 1987, 1988) is covalently blocked by a cyt.c molecule in complex 3. Therefore, by testing the ability of complexes 2 and 3 to oxidize exogenous ferrocyt.c in the steady state reaction, we can gain insight on whether important sites of interaction are masked. We therefore measured the steady state activities of complexes 2 and 3 upon addition of exogenous yeast or horse ferrocyt.c at different ionic strengths. The conditions used for these experiments were similar to the those already optimized by Wang and Margoliash (1995).

The Eadie−Hofstee plots for horse heart or yeast ferrocyt.c at different ionic strengths are presented in Figures 5 and 6 and summarized in Table 1. The characteristic biphasic behavior has been attributed to two ferrocyt.c binding sites (Kang et al., 1977). Using horse heart ferrocyt.c as the substrate, complex 3 exhibits activity comparable to that of A128CCP but complex 2 has very low activity in both 1 and 5 mM buffers (Figure 5, Table 1). This observation indicates that the site(s) for horse heart ferrocyt.c is still available in complex 3 but blocked in complex 2. Using yeast ferrocyt.c as substrate, wild type CCP and both complexes exhibit very low activity at low ionic strengths, as expected (Wang & Margoliash, 1995; inset of Figure 6). At higher ionic strengths, 100 mM Tris, complex 3 exhibits activity comparable to that of wild type CCP but complex 2 exhibits very low activity (Figure 6, Table 1). This indicates that in complex 2 the site of electron transfer for yeast ferrocyt.c at high ionic strengths is blocked.

DISCUSSION

Probing Interaction Domains. The method of site specific cross-linking where two redox partners are tethered through an engineered disulfide was developed (Pappa & Poulos, 1995) for two reasons. The first of these is to probe interaction domains in an attempt to identify the expected second site of interaction in the CCP−cyt.c system. The

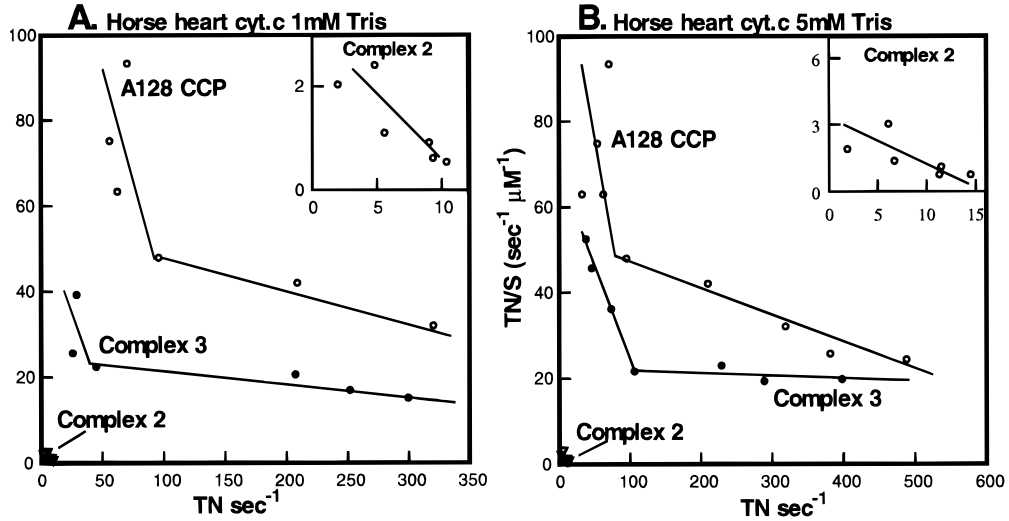

FIGURE 5: Eadie−Hofstee plots of the various enzymes using horse heart ferrocyt.c as susbtrate at the indicated buffer concentrations. The experimental conditions used are described in Materials and Methods.

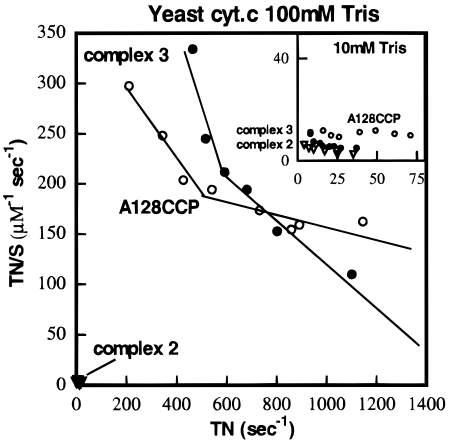

FIGURE 6: Eadie−Hofstee for the various enzymes using yeast ferrocyt.c as the substrate in 100 mM Tris buffer. The inset shows the Eadie−Hofstee plots in 10 mM Tris buffer. The experimental conditions used are described in Materials and Methods.

second is to test the role of the pathway versus distance models of electron transfer. First, we consider the question of interaction domains. Recent mutagenesis studies designed to probe the interaction domain(s) between CCP and cyt.c are consistent with the Pelletier−Kraut model as a functionlly relevant complex (Miller et al., 1994). Moreover, in our previous work (Pappa & Poulos, 1995), complex 2 was designed to mimic the Pelletier−Kraut structure and was found to exhibit an intramolecular electron transfer rate similar to what has been observed in the noncovalent complex. This observation, together with the fact that changing Trp191 to Phe eliminates electron transfer in complex 2 just as it does in the noncovalent complex (Mauro et al., 1988), supports the view that complex 2 and the crystal structure of the noncovalent complex (Pelletier & Kraut, 1992) are very similar and represent one of the primary electron transfer competent sites. Wang and Margoliash (1995) have carried out a similar study by cross-linking cyt.c to CCP using a photoactive cross-linking group attached to an engineered cysteine residue in cyt.c. Although the site of attachment to CCP is unknown in these complexes, their activity profiles indicate that the cyt.c occupies the high-affinity site of CCP. In a similar way, complex 2 is inactive toward exogenous horse heart ferrocyt.c at both low and high ionic strengths and exogenous yeast ferrocyt.c at high ionic strength. However, complex 2 does exhibit about 40−50% of wild type levels of activity toward yeast ferrocyt.c at low ionic strengths. Some of the cross-linked complexes prepared by Wang and Margoliash (1995) are likely tethered in an orientation similar to our complex 2 which, in turn, is very likely the same as that observed in the crystal structure of the noncovalent complex (Pelletier & Kraut, 1992).

To summarize, the steady state results indicate that in complex 2 the primary and perhaps only functionally important site for interaction with horse heart ferrocyt.c is blocked. However, for yeast ferrocyt.c, a second site remains open in complex 2 at low ionic strengths. This still leaves open the question regarding the location of the second site. Using Brownian dynamics methods, Northup et al. (1987, 1988) provided an estimate on the location of this second site, centered on Asp148 of CCP. Complex 3 was designed to block this site. The steady state results using yeast ferrocyt.c as the substrate show that complex 3 behaves very much the same as wild type CCP. Indeed, the biphasic nature of the Eadie−Hofstee plots and levels of activity are very similar. This indicates that both cyt.c binding sites are still available in complex 3, further indicating that the region of CCP centered near Asp148 is unlikely to be a catalytically competent site of interaction.

Distance versus Pathway Models of Electron Transfer. In the pathway model, electron transfer occurs along preferred routes through the protein (Winkler & Gray, 1992), while in the distance model, the distance between redox centers is the primary factor controlling rates (Moser et al., 1992). Assuming that the heme−heme or iron−iron distance is most relevant, then by moving cyt.c to different regions on CCP yet holding the heme−heme edge distance constant, we should be able to gain insight on the relative roles of distance versus pathway. In modeling complex 3, the C149CCP-to-C79cyt.c disulfide holds the heme edges 14−18 Å apart and the iron atoms 22−25 Å apart, independent of the precise orientation between cyt.c and CCP compared to 19 and 26 Å, respectively, in the crystal of the noncovalent complex (Pelletier & Kraut, 1992). Therefore, if the heme−heme edge or iron−iron distance is important, the intramolecular electron transfer rate in complexes 2 (which was designed to mimic the crystal structure) and 3 will be similar. This

Table 1: The Activity of CCP where the Naturally Occurring Cys128 Was Converted to Ala, A128CCP, Is Taken as 100

	0.7 μM yeast cyt.c and 10 mM Tris (pH 7.0)	5.6 μM yeast cyt.c and 10 mM Tris (pH 7.0)	1.4 μM yeast cyt.c and 100 mM Tris (pH 7.0)	7 μM yeast cyt.c and 100 mM Tri (pH 7.0)
A128CCP	100	100	100	100
complex 2	29.6 ± 1.5	14 ± 1.7	1.3 ± 0.15	1.3 ± 0.15
complex 3	95.1 ± 4.0	45 ± 2.0	108 ± 12	75.3 ± 3.0

	1 μM horse cyt.c and 1 mM Tris (pH 7.0)	10 μM horse cyt.c and 1 mM Tris (pH 7.0)	1 μM horse cyt.c and 5 mM Tris (pH 7.0)	10 μM horse cyt.c and 5 mM Tris (pH 7.0)
A128CCP	100	100	100	100
complex 2	3 ± 0.1	3.1 ± 0.15	2.8 ± 0.1	3.6 ± 0.05
complex 3	51 ± 10.0	67.3 ± 10.0	75.7 ± 10.0	72.0 ± 4.0

is not the case because intramolecular electron transfer occurs about 3 orders of magnitude more slowly in complex 3. However, the stopped flow results show that our initial assumption that the heme−heme or iron−iron distance is the most important one to consider may not be valid. The more relevant distance is cyt.c heme−Trp191 because it is the Trp191 radical that is reduced by ferrocyt.c in both complexes 2 and 3.

Reduction of the Trp191 radical in complex 3 was unexpected because the cyt.c heme should be closer to the CCP heme than to Trp191, 14−18 versus 20−23 Å. The cyt.c heme−Trp191 distance in the Pelletier−Kraut structure is 16 Å so the maximum difference in this distance between complex 3 and the Pelletier−Kraut structure is 7 Å. Can a 7 Å distance account for the approximately 1000-fold decrease in the intramolecular electron transfer rate of complex 3 compared to that of complex 2? We can gain some insight on this question by using Marcus theory (Marcus & Sutin, 1985). A simplified empirically derived version of the theory has been developed by Dutton and colleagues (Moser et al., 1992; Farid et al., 1993), where the electron transfer rate (in s^{-1}) is given by

$$\log k_{et} = 15.2 - 0.61R - 3.1(\Delta G - \lambda)^2/\lambda$$

R is the donor−aceeptor distance, ΔG is the driving force of the reaction, and λ is the reorganization energy. Because the metal centers are not altered in these complexes, we take ΔG and λ to be constants. Even if λ changes by a factor of 2, the change in rate will not be very large, and the primary dependence is on R, the donor−acceptor distance. Given these assumptions, the 7 Å distance increase leads to an expected rate difference of about 10^4, while the experimentally determined difference has a lower estimate of 10^3.

If this were the only information available, we might conclude that distance is what controls rate. The Trp191 radical, however, is reduced in complex 2 even though the heme groups are closer to each other than the cyt.c heme is to Trp191. This observation is opposite to what is expected if distance controls rate. Another possibility is that the Trp191 radical is a more potent oxidant. Information regarding the relative stability of the Fe^{4+}═O center and the Trp191 radical is available. At pH 6.0, the pH where our studies are carried out, the ratio [Fe^{3+} Trp•]:[Fe^{4+} Trp] is estimated to be 0.54 (Coulson et al., 1971) and 0.36 (Hahm et al., 1994). Therefore, at pH 6.0, the Fe^{4+}═O center is more stable than the Trp radical. However, this stability difference is small (<1 kcal/mol), and therefore, there must be some other reason for the preferred reduction of the Trp191 radical.

Another possibility to explain the preference for Trp191 radical reduction is based on the following mechanism (Hahm et al., 1994):

$$CCP(Fe^{4+}{=}O\ Trp^{\bullet}) + e^- \rightarrow CCP(Fe^{4+}{=}O\ Trp) \rightarrow CCP(Fe^{3+}\ Trp^{\bullet})$$

$$CCP(Fe^{3+}\ Trp^{\bullet}) + e^- \rightarrow CCP(Fe^{3+}\ Trp)$$

In this mechanism, only the Trp191 radical receives an electron from ferrocyt.c, which requires intramolecular electron transfer from Trp191 to the Fe^{4+}═O center. The main problem with this picture is the apparent very slow reduction of the CCP Fe^{4+}═O center by Trp191 (Ho et al., 1983)m although Ho et al. (1983) proposed that, under steady state conditions, Trp191 is present in a form that can reduce Fe^{4+}═O. This mechanism would be favored if reduction of both the Trp191 radical and Fe^{4+}═O is initiated at the same site on the CCP surface. Previous stopped flow studies, however, show that Fe^{4+}═O is reduced first at low ionic strengths but that the radical is reduced first at high ionic strengths (Hahm et al., 1993; Matthis et al., 1995). This could mean that reduction of both centers still occurs at the same site but that the [Fe^{3+} Trp•]:[Fe^{4+} Trp] equilibrium is quite sensitive to ionic strength and that the equilibration between the two centers is fast compared to the electron transfer from ferrocyt.c. Alternatively, there are two sites. One site favors Fe^{4+}═O reduction, and the other favors Trp191 radical reduction (Zhou & Hoffman, 1993, 1994; Mauk et al., 1994). Taken together, our data favor the pathway model because Trp191 is essential in complex 2. Nevertheless, control of biological electron transfer reactions is more complex than our simple analysis of pathway versus distance might imply. For example, the orientation of the donor−acceptor pair and the symmetry of corresponding wave functions have a significant influence on the path of electron transfer (Stuchebrukhov & Marcus, 1995). However, because of covalent tethering of cyt.c to CCP in structurally defined complexes, as in complex 2, it now is possible to address the factors controlling intramolecular electron transfer in the CCP−cyt.c complex.

Summary. Our results provide further evidence that complex 2 is very similar to the Pelletier−Kraut model for the noncovalent complex and that this complex is efficient in intramolecular electron transfer. The Trp191 radical is essential for oxidation of ferrocyt.c in complex 2 which means that CCP has a second site for reducing Fe^{4+}═O or that Trp191 rapidly reduces Fe^{4+}═O. That complex 2 retains activity toward exogenous ferrocyt.c at low ionic strengths

supports the view that CCP has a second site for electron transfer. It should be emphasized, however, that this second site may not be physiologically relevant because *in vivo* CCP operates in a high-ionic strength milieu (Pettigrew & Moore, 1987). This work also shows that, in testing the pathway versus distance models of electron transfer, the relevant distance is the cyt.c heme−CCP Trp191 distance and not just the heme−heme or iron−iron distance. Finally, the high steady state activity of complex 3 indicates that the proposed second electron transfer site centered on Asp148 of CCP is unlikely to represent one of the regions important for electron transfer.

REFERENCES

Choudhury, K., Sundaramoorthy, M., Hickman, A., Yonetani, T., Woehl, E., Dunn, M. F., & Poulos, T. L. (1994) *J. Biol. Chem. 269*, 20239−20249.

Coulson, A. F. W., Erman, J. E., & Yonetani, T. (1971) *J. Biol. Chem. 246*, 917−924.

Cutler, R. L., Pielak, G. J., Mauk, A. G., & Smith, M. (1987) *Protein Eng. 1*, 95−99.

Erman, J. E., & Vitello, L. B. (1980) *J. Biol. Chem. 255*, 6224−6227.

Erman, J. E., Kim, K. L., Vitello, L. B., Moench, S. J., & Saterlee, J. D. (1987) *Biochim. Biophys. Acta 911*, 1−10.

Erman, J. E., Vitello, L. B., Mauro, J. M., & Kraut, J. (1989) *Biochemisty 28*, 7992−7995.

Farid, R. S., Moser, C. C., & Dutton, P. L. (1993) *Curr. Opin. Struct. Biol. 3*, 225−233.

Fishel, L. A., Villafranca, J. E., Mauro, J. M., & Kraut, J. (1987) *Biochemistry 26*, 351−360.

Geren, L., Hahm, S., Durham, B., & Millett, F. (1991) *Biochemistry 30*, 9450−9457.

Hahm, S., Geren, L., Durham, B., & Millett, F. (1993) *J. Am. Chem. Soc. 115*, 3372−3373.

Hahm, S., Miller, M. A., Geren, L., Kraut, J., Durham, B., & Millett, F. (1994) *Biochemistry 33*, 1473−1480.

Hazzard, J. T., Poulos, T. L., & Tollin, G. (1987) *Biochemistry 26*, 2836−2848.

Hilgen, S. E., & Pielak, G. J. (1991) *Protein Eng. 5*, 575−578.

Kang, C. H., Ferguson-Miller, S., & Margoliash, E. (1977) *J. Biol. Chem. 252*, 919−926.

Kunkel, T. A., Roberts, J. D., & Zokour, R. A. (1987) *Methods Enzymol. 154*, 367−382.

Leonard, J. J., & Yonetani, T. (1974) *Biochemistry 13*, 1465−1468.

Marcus, R. A., & Sutin, N. (1985) *Biochim. Biophys. Acta 811*, 265−322.

Matthis, A. L., Vitello, L. B., & Erman, J. E. (1995) *Biochemistry 34*, 9991−9999.

Mauk, M. R., Ferrer, J. C., & Mauk, A. G. (1994) *Biochemistry 33*, 12609−12614.

McLendon, G., Zhang, Q., Wallin, S. A., Miller, R. M., Billstone, V., Spears, K. G., & Hoffman, B. M. (1993) *J. Am. Chem. Soc. 115*, 3665−3669.

Miller, M. A., Liu, R.-Q., Hahm, S., Geren, L., Hibdon, S., Kraut, J., Durham, B., & Millett, F. (1994) *Biochemistry 33*, 8686−8693.

Mochan, E. (1970) *Biochim. Biophys. Acta 216*, 80−95.

Mochan, E., & Nicholls, P. (1971) *Biochem. J. 121*, 69−82.

Mochan, E., & Nicholls, P. (1972) *Biochim. Biophys. Acta 267*, 309−319.

Moench, S. J., Chroni, S., Lou, B., Erman, J. E., & Satterlee, J. D. (1992) *Biochemistry 31*, 3661−3670.

Moser, C. C., Keske, J. M., Warncke, K., Farid, R. S., & Dutton, P. L. (1992) *Nature 355*, 796−802.

Northrup, S. H., Boles, J. O., & Reynolds, J. C. L. (1987) *J. Phys. Chem. 91*, 5991−5998.

Northrup, S. H., Boles, J. O., & Reynolds, J. C. L. (1988) *Science 241*, 67−70.

Onuchic, J. N., & Beratan, D. N. (1990) *J. Chem. Phys. 92*, 722−733.

Pappa, H. S., & Poulos, T. L. (1995) *Biochemistry 34*, 6573−6580.

Pelletier, H., & Kraut, J. (1992) *Science 258*, 1748−1755.

Pettigrew, G. W., & Moore, G. R. (1987) *Cytochrome c: Biological Aspects*, pp 95−96, Springer-Verlag, Berlin.

Poulos, T. L., & Kraut, J. (1980) *J. Biol. Chem. 255*, 10322−10330.

Richarson, J. S. (1981) *Adv. Protein Chem. 34*, 167−339.

Sivaraja, M., Goodin, D. B., Smith, M., & Hoffman, B. M. (1989) *Science 245* 738−740.

Stemp, E. D. A., & Hoffman, B. M. (1993) *Biochemistry 32*, 10848−10865.

Stuchebrukhov, A. A., & Marcus, R. A. (1995) *J. Chem. Phys. 99*, 7581−7590.

Thornton, J. M. (1981) *J. Mol. Biol. 151*, 261−287.

Waldmeyer, B., & Bosshard, H. R. (1985) *J. Biol. Chem. 260*, 5184−5190.

Wang, Y., & Margoliash, E. (1995) *Biochemistry 34*, 1948−1958.

Winkler, J. R., & Gray, H. B. (1992) *Chem. Rev. 92*, 369−379.

Yi, Q., Erman, J. E., & Satterlee, J. D. (1993) *Biochemistry 32*, 10988−10994.

Yonetani, T. *The Enzymes* (Boyer, P. D., Ed.) Vol. 13, Chapter 6, pp 345−361, Academic Press, Orlando, FL.

Zhou, J. S., & Hoffman, B. M. (1994) *Science 265*, 1693−1696.

Zhou, J. S., & Hoffman, B. M. (1995) *Science 269*, 204−207.

BI952935B